Triaxial-Stress-Induced Homogeneous Hysteresis-Free First-Order Phase Transformations with Stable Intermediate Phases

Valery I. Levitas,[1,2] Hao Chen,[3] and Liming Xiong[3]

[1]*Iowa State University, Departments of Aerospace Engineering, Mechanical Engineering,*
and Material Science and Engineering, Ames, Iowa 50011, USA
[2]*Ames Laboratory, Division of Materials Science and Engineering, Ames, Iowa 50011, USA*
[3]*Iowa State University, Department of Aerospace Engineering, Ames, Iowa 50011, USA*
(Received 20 September 2016; published 11 January 2017)

Starting with thermodynamic predictions and following with molecular dynamics simulations, special triaxial compression-tension states were found for which the stresses for the instability of the crystal lattice of silicon (Si) are the same for direct and reverse phase transformations (PTs) between semiconducting Si I and metallic Si II phases. This leads to unique homogeneous and hysteresis-free first-order PTs, for which each intermediate crystal lattice along the transformation path is in indifferent thermodynamic equilibrium and can be arrested and studied by fixing the strain in one direction. By approaching these stress states, a traditional two-phase system continuously transforms to homogenous intermediate phases. Zero hysteresis and homogeneous transformations are the optimal property for various PT applications, which drastically reduce damage and energy dissipation.

First-order displacive stress-induced phase transformations (PTs) under normal and high pressure are of great fundamental and applied interest for the synthesis and application of new phases and materials [1–7]. PTs start when the crystal lattice of a parent phase loses its stability [1,8]. Stresses for direct and reverse PTs are located on different sides of the phase equilibrium stress (see Ref. [8] and Fig. 1), and their difference represents stress hysteresis, which can be quite large. Any intermediate homogeneous state of the crystal lattice along the transformation path is unstable under prescribed stresses. If strain is prescribed or fixed during transformation in an attempt to stabilize intermediate state, the material transforms into a hetero-geneous two-phase system [similar to Fig. 2(a)] with interfaces between the phases (nucleation), and further growth of the product phase occurs via interface motion. In real materials, defects produce stress concentrations and instabilities start locally near defects at smaller deviation from the equilibrium stresses. Because of lattice mismatch, interfaces generate significant elastic stresses, that propagate together with interfaces through the entire sample during cyclic direct-reverse PTs and cause damage while passing through material defects. Stress hysteresis for growth is determined by interfacial friction and energy [2,9]. On the applied side, stress hysteresis and the corresponding energy dissipation, as well as interfacial stresses should be reduced for many PT-related applications, like for shape memory alloys for actuation or medical applications [2–4] or caloric materials [4,5]. On the fundamental side, it is of interest to stabilize intermediate structures along the transformation path and study their properties [10], with the expectation that they may be unique. Also, significant reduction of the PT pressure by applying nonhydrostatic stresses is of basic and

applied interests [1,6,7], but it is still not connected to lattice instabilities.

Let us consider, as an example, a cubic crystal lattice under action of three stresses normal to cubic faces, σ_i, and for compactness assume $\sigma_1 = \sigma_2 \neq \sigma_3$. Let lattice instability
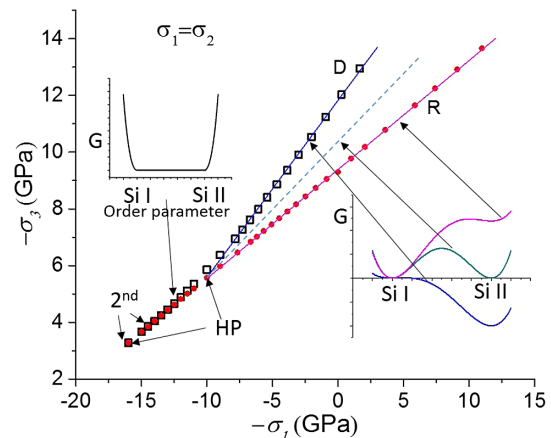

FIG. 1. Relationships between stresses σ_3 and $\sigma_1 = \sigma_2$ for crystal lattice instability for direct and reverse Si I ↔ Si II PTs and the existence of the continuum of homogenous intermediate phases. Each instability line is related to the disappearance of the minimum in the Gibbs energy G plot for the corresponding phase. The dashed line is the tentative phase equilibrium line corre-sponding to equality of the Gibbs energy G of phases. For stress states at the merge of two instability lines, Gibbs energy has a plateau with constant value leading to a unique homogeneous and hysteresis-free first-order Si I ↔ Si II PT, with a continuum of intermediate homogeneous phases (HPs), which are in indifferent thermodynamic equilibrium. With a further increase in σ_1, the first-order transformation changes to the second-order transition (designated as 2nd) and then (not shown) to a disordered phase.
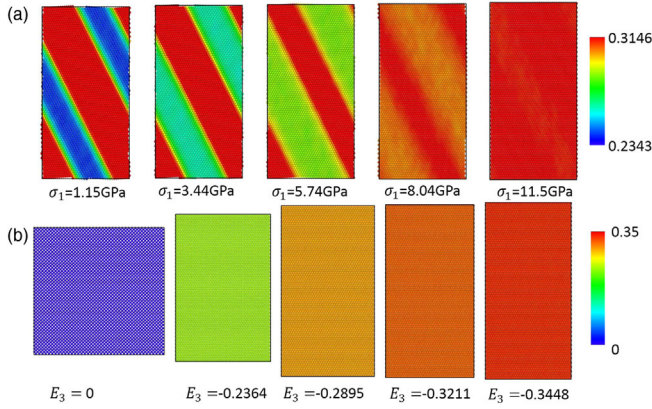
FIG. 2.   Nanostructure evolution in silicon during phase transformation. (a) Transformation of two-phase Si I-Si II mixture into intermediate homogeneous phases at prescribed compressive Lagrangian strain $E_3 = -0.31$ and increasing tensile stresses $\sigma_1 = \sigma_2$. (b) Homogeneous transformation process from Si I to Si II through continuum of homogeneous phases with increasing strain E_3 at fixed stresses $\sigma_1 = \sigma_2 = 11$ GPa. Colors characterize the local von-Mises shear strain.

lines in the plane $\sigma_1 - \sigma_3$ have different slopes for direct and reverse first-order PTs, see the example for Si I $\leftrightarrow$ Si II PTs in Fig. 1. Instability lines correspond to the disappearance of the respective minimum of the Gibbs energy G (Fig. 1), where the order parameter is related to the transformation strain that transforms the crystal lattice of the parent phase to that of the product phase [8,11,12]. Since instability lines have different slopes, they should have a common point. They cannot intersect, i.e., be continued beyond the common point, because this would mean that the low stress (pressure) phase transforms to the high pressure phase at a stress reduction, which is contradictory. We exclude the cases where the common point represents transition from the first- to second-order PT or critical point, beyond which phases are not distinguishable. Then the lattice instability lines should merge for some range of stresses (Fig. 1). The phase equilibrium line [corresponding to the equality of the Gibbs energy of phases (Fig. 1)] is between instability lines, and consequently, it should also coincide with the merged lines. Stress hysteresis, which is defined as the difference in values of σ_3 between instability stresses for direct and reverse PTs for the same σ_1, decreases to zero when σ_1 tends toward the merged region. Within the merged region, the energy barrier between phases disappears and the Gibbs energy possesses a flat portion (Fig. 1) with the constant energy between strains corresponding to each of the phases. Consequently, each intermediate phase along the transformation path has the same Gibbs energy as both phases and is by definition in a neutral or indifferent (i.e., intermediate between stable and unstable) thermodynamic equilibrium state. This should lead to unique homogeneous and hysteresis-free first-order PTs. Each of the states can be considered as a separate intermediate phase since it has distinct lattice parameters and the transformation between any of these states

is accompanied by a change in strain and latent heat. Thus, there is an infinite number (continuum) of intermediate phases with homogeneous (without interfaces) transformations between them. These intermediate homogeneous phases and the entire transformation process can be arrested and studied by fixing strain in one direction; they may possess exceptional properties. When starting with a two-phase structure, stresses change toward the merged region, the energy barrier between phases at equilibrium, $A \to 0$. In continuum Ginzburg-Landau-type theory [8,11,12], the interface energy is $\sim \sqrt{A}$, and the width is $\sim 1/\sqrt{A}$. Thus, when approaching the merged region, the interface energy tends to zero but width diverges. This means the two-phase structure should continuously transform to a homogenous intermediate phase. Before reaching homogeneous states, unique heterogeneous intermediate structures with very broad interfaces with controllable width can also be stabilized at a prescribed strain. These structures may possess unexpected properties. Because of homogeneous transformation and lack of interfaces, internal stresses are absent and damage will be minimal as well, despite the possibility of large transformation strains. Zero hysteresis results in zero energy dissipation. Both these properties are of great fundamental interest and applied importance for various PT-related applications [2–5]. These phenomena should occur for any known or specially designed material for which stresses for the instability of crystal lattice can be made the same for direct and reverse PTs.

   The above hypothetical scenario is purely thermodynamic and is not related to any specific atomic structure. The goal of the current Letter is to find a proof of concept for the above described behavior. This can be done using phase field or atomistic simulations. For a small sample consisting of a dozen lattice cells under strain-controlled condition, transformation is always homogeneous even when there is a barrier between phases [13–15]. This is a well-known size effect, which does not allow a heterogeneous microstructure in a small sample because of interfacial and elastic energy. Thus, a sample should have large enough size and size independence of the observed phenomena should be proven. First principles simulations are prohibitively expensive for such simulations, so we chose molecular dynamics (MD). In principle, any interatomic potential would be sufficient for the proof of concept, even a Lennard-Jones potential. To make it more realistic, we consider here Si I $\leftrightarrow$ Si II PTs using the Tersoff potential (see Supplemental Material [16]).

   MD simulations at 1 K were utilized to study PTs Si I $\leftrightarrow$ Si II under various combinations of compressive true (Cauchy) stress (i.e., force per unit deformed area) σ_3 and two normal stresses $\sigma_1 = \sigma_2$, all along cubic axes (Fig. 1); positive stresses are tensile. Lattice instability and initiation of PT correspond to stresses at which the initial crystal lattice cannot be stabilized. It is found that in the $\sigma_3 - \sigma_1$ plane initiation of both direct and reverse PTs occurs at straight lines (Fig. 1), described by equations

$\sigma_3^d = -11.8286 + 0.6240\sigma_1$ and $\sigma_3^r = -9.3888 + 0.3840\sigma_1$. Because instability lines possess different slopes, they should intersect at the point $\sigma_1 = 10.1658$ and $\sigma_3 = -5.4851$. Instead, the instability line for the Si I → Si II PT bends and merges with the line for the Si II → Si II PT within a broad stress range, in agreement with our predictions. When stresses $\sigma_1 = \sigma_2 = 11$ GPa were fixed at a value corresponding to the zero-barrier region, an increase in compressive Lagrangian strain E_3 (i.e., increase of the displacement at the boundary) leads to the homogeneous transformation process from Si I to Si II, and an intermediate crystal structure can be arrested [see Fig. 2(b) and Supplemental videos 1 and 3–5]. Away from the merged region, when Si I loses its stability, transformation occurs through nucleation of Si II followed by formation of Si II bands [like in Fig. 2(a) and video 2] and their growth until completing the PT. This happens both under prescribed stresses and prescribed and changing strains; i.e., homogeneous intermediate structures are not observed and cannot be stabilized away from the zero-barrier region.

When we start with a two-phase structure under fixed strain E_3 and increase tensile stresses $\sigma_1 = \sigma_2$ toward the merged region, the two-phase Si I-Si II structure continuously transforms with increasing σ_1 to the intermediate homogenous phase [Fig. 2(a) and movie 3] that is determined by E_3. When starting with a homogeneous intermediate phase and reducing tensile stress $\sigma_1 = \sigma_2$, the same structures are observed at the same stresses (movie 4); i.e., the transformation process is fully reversible without hysteresis. Presence of two-phase structure and continuous transition to and from it from and to homogeneous intermediate structures, the same for sample sizes from 5 to 40 nm, prove that the homogeneous transformation is not caused by small sample size and/or periodic boundary conditions. Thus, all our thermodynamic predictions have been confirmed for Si I ↔ Si II PTs, which occur at large elastic and transformational strains.

An additional insight can be obtained by analyzing stress-strain curves for Si I ↔ Si II PTs in Fig. 3, which are the same for increasing and decreasing strains E_3. In the stress σ_1 range 10–13 GPa, some small differences between instability stresses for direct and reverse PTs are observed, but they are within ±1%, which is below the simulation error. That is why we claim that both instability lines in Fig. 1 merge within a finite stress σ_1 range. Strain distribution within the instability region is homogeneous for $\sigma_1 \geq 10$ GPa and for each E_3 describes intermediate homogeneous phase.

With increasing stress σ_1, the difference in strain for initiation of the direct and reverse PTs reduces and reaches zero at 14 GPa, which substitutes the first-order PT with the second order PT (Fig. 3 and movie 6). In contrast to known second-order PTs, which are related to the shift of intracell atoms and corresponding change in symmetry and occur at small strains, here there are no intracell atomic displacements [Fig. 4(a)] and changes in symmetry, and strains are very
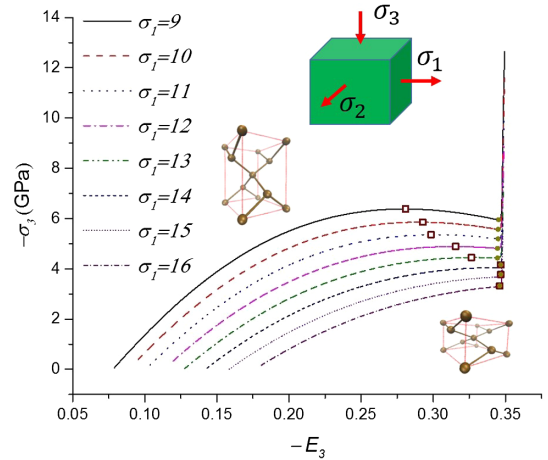

FIG. 3. True stress σ_3 versus Lagrangian strain E_3 for various fixed stresses $\sigma_1 = \sigma_2$ and increasing or decreasing E_3 during Si I ↔ Si II PT. Lattice instability points for Si I → Si II PT correspond to the local maxima of stresses while for Si II → Si I PT they correspond to the local minima. Between them, the transformation path passes through the continuum of intermediate homogeneous phases.

large. This second-order PT only represents a large jump in elastic modulus. A further increase in σ_1 leads to disordered phase, which will be discussed elsewhere.

The possibility of arresting intermediate homogeneous phases, if confirmed by experiments, opens unprecedented opportunities to study their properties and the entire transformation process. For example, how do semiconducting properties change to metallic ones and at what stage? What are the structures with intermediate semiconducting-metallic states? What are the thermodynamic and mechanical properties of intermediate states that participate in Landau-type theory for stress-induced displacive PTs [8,12]? There was never a way to determine them directly experimentally. Intermediate homogeneous phases may exhibit some unknown and extraordinary properties, which could find corresponding applications.
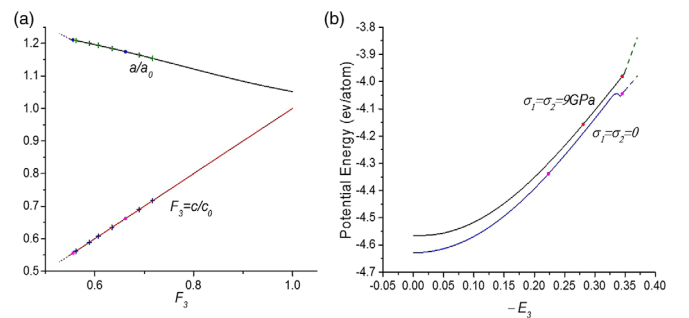

FIG. 4. Properties of locally unstable intermediate homogeneous phases. Bold dots designate instability points. (a) Components of deformation gradient $F_3 = c/c_0$ and $F_1 = a/a_0$ for $\sigma = 9$ GPa vs F_3. Lines are based on crystal cell parameters and symbols are calculated based on the intracell atoms. (b) Potential energy versus F_3 for two different stresses σ_1.

Note that homogeneous strain was also observed for $\sigma_1 = 9$ GPa (Supplemental video 5) and the stress-strain curve shown in Fig. 3 is the same for sample sizes from 5 to 40 nm. Since there is a small but finite Gibbs energy barrier between Si I and Si II, these intermediate homogeneous phases are not in indifferent equilibrium. Even better, it shows the possibility to stabilize intermediate locally unstable homogeneous phases, including the phase corresponding to the local energy maximum. The alternative two-phase structure is suppressed due to interfacial energy and the energy of internal elastic stresses. At the lower stress $\sigma_1 = 8$ GPa the intermediate heterogeneous nanostructure is stabilized (Supplemental video 2), in which strain oscillates with the magnitude of 5% without clear phases and interfaces. At $\sigma_1 = 6.9$ GPa, intermediate low-strain phase is (almost) homogeneous but the high-strain phase region is much thinner than the interface region and does not possess homogenous-strain portion. Again, our thermodynamic prediction of slightly heterogeneous intermediate structures and structures with broad interfaces is confirmed with MD simulations. Stabilized intermediate heterogeneous states may also possess interesting properties.

Figure 4 presents some properties of intermediate homogeneous phases. Components of the deformation gradients $F_3 = c/c_0$ and $F_1 = a/a_0$, where c and a are the lattice parameters of the deformed tetragonal cell and subscript 0 corresponds to the unstrained initial lattice ($a_0 = c_0$), are presented in Fig. 4(a). Interestingly, that linear relationship for F_1 for intermediate phases is just a smooth linear continuation of the curve for Si I, despite the large strains and nonlinear elasticity. When F_1 and F_3 were calculated based on the intracell atoms, results were the same. That means that the Cauchy-Born hypothesis is met; i.e., intracell atoms do not have independent degrees of freedom; consequently, they cannot cause instability for first- and second-order PTs. The potential energy of the system vs strain E_3 is presented in Fig. 4(b). While for $\sigma_1 = 0$ GPa this is the energy of the mixture of Si I and Si II, for $\sigma_1 = 9$ GPa this is the energy of the locally unstable intermediate homogeneous phases. Linear energy vs E_3 corresponds to constant energetic stress.

We also found that if one varies $\sigma_2 \neq \sigma_1$ keeping $\sigma_2 + \sigma_1 = $ const, this practically does not affect σ_3^d or σ_3^r. This significantly broadens the stress states for which intermediate homogeneous phases and hysteresis-free PT can occur.

To summarize, we predicted thermodynamically and proved with MD simulations for Si I $\leftrightarrow$ Si II PTs new phenomenon of homogeneous and hysteresis-free first-order PT. A broad range of special triaxial compression-tension states was found for which the stresses for the lattice instability for direct and reverse PTs were the same. Since the energy barrier between two phases disappears, and the Gibbs energy landscape has a constant flat region, each intermediate state along the transformation path is in a neutral thermodynamic equilibrium and can be considered

as a separate intermediate phase. Thus, there is a continuum of the intermediate phases with homogeneous and hysteresis-free transformations between them. Each intermediate phase can be arrested and studied by fixing the strain in one direction. By approaching these stress states, the interface width in a traditional two-phase system increases and diverges, interface energy tends to zero, and a two-phase structure continuously transforms to homogenous intermediate phases. This also allows for the stabilization of unique slightly heterogeneous intermediate structures with broad and controlled interface widths, which may possess unexpected properties. As it was found in Refs. [33–37], the ratio of the thickness of widths of two different phase interfaces drastically affects nano- and macroscale transformational properties for various PTs. Thus, multiaxial stresses may allow us to vary this ratio in a broad range, producing new properties and phenomena. Zero hysteresis and homogeneous transformations are the optimal property for various PT-related applications [2–5], which reduce damage and energy dissipation. Further increases in stresses substitute the first-order PT with the unusual second-order PT, without intracell atomic displacements and change in symmetry, and at large strains.

While it is well-known that utilization of first principles simulations instead of MD would deliver more reliable results for Si and other materials, our results are sufficient for conceptual proof. Similar phenomena and phases may be found in many other materials. Since there is no fundamental reason for collinearity of the instability lines, they should intersect for many material systems. The practical problem is whether this region is achievable before fracture or plastic flow occurs. Materials in which homogenous PTs may occur could be designed by proper multicomponent alloying, as was done for shape memory alloys [2–4] or caloric materials [4,5]. Multiaxial loading can be combined with other stimuli, like temperature and magnetic field, which will increase the chances to find zero-hysteresis transformations and intermediate homogeneous phases for economically realistic external stimuli. If confirmed by experiments, these results will allow one to control or reduce the stress hysteresis, interface energy and dissipation, and reduce damage by controlling the multiaxial stress state and other fields, which may revolutionize the field of transforming materials, in particular, for elastocaloric and smart material applications.

[1] V. D. Blank and E. I. Estrin, *Phase Transitions in Solids under High Pressure* (CRC Press, Boca Raton, 2014), pp. 382–423.

[2] J. Cui *et al.*, Combinatorial search of thermoelastic shape memory alloys with extremely small hysteresis width, Nat. Mater. **5**, 286 (2006).

[3] C. Chluba, W. Ge, R. Lima de Miranda, J. Strobel, L. Kienle, E. Quandt, and M. Wuttig, Ultralow-fatigue shape memory alloy films, Science **348**, 1004 (2015).

[4] S. Yintao, C. Xian, V. Dabade, T. W. Shield, and R. D. James, Enhanced reversibility and unusual microstructure of a phase transforming material, Nature (London) **502**, 85 (2013).

[5] I. Takeuchi and K. Sandeman, Solid-state cooling with caloric materials, Phys. Today **68**, No. 63, 48 (2015).

[6] V. I. Levitas and L. K. Shvedov, Low pressure phase transformation from rhombohedral to cubic BN: Experiment and theory, Phys. Rev. B **65**, 104109 (2002).

[7] C. Ji, V. I. Levitas, H. Zhu, J. Chaudhuri, A. Marathe, and Y. Ma, Shear-induced phase transition of nanocrystalline hexagonal boron nitride to wurtzitic structure at room temperature and lower pressure, Proc. Natl. Acad. Sci. U.S.A. **109**, 19108 (2012).

[8] V. I. Levitas and D. L. Preston, Three-dimensional Landau theory for multivariant stress-induced martensitic phase transformations. Part II. Multivariant phase transformations and stress space analysis, Phys. Rev. B **66**, 134207 (2002).

[9] G. Ghosh and G. B. Olson, Kinetics of F.C.C. -> B.C.C. heterogeneous martensitic nucleation—I. The critical driving force for athermal nucleation, Acta Metall. Mater. **42**, 3361 (1994).

[10] A. van de Walle, Q. Hong, S. Kadkhodaei, and R. Sun, The free energy of mechanically unstable phases, Nat. Comput. **6**, 7559 (2015).

[11] V. I. Levitas, D.-W. Lee, and D. L. Preston, Phase field theory of surface- and size-induced microstructures, Europhys. Lett. **76**, 81 (2006).

[12] V. I. Levitas, Phase field approach to martensitic phase transformations with large strains and interface stresses, J. Mech. Phys. Solids **70**, 154 (2014).

[13] S. Sorella, M. Casula, L. Spanu, and A. Dal Corso, Ab initio calculations for the β-tin diamond transition in silicon: Comparing theories with experiments, Phys. Rev. B **83**, 075119 (2011).

[14] R. Maezono, N. D. Drummond, A. Ma, and R. J. Needs, Diamond to β-tin phase transition in Si within diffusion quantum Monte Carlo, Phys. Rev. B **82**, 184108 (2010).

[15] S. L. Qiu and P. M. Markus, Equilibrium lines and barriers to phase transitions: the cubic diamond to β-tin transition in Si from first principles, J. Phys. Condens. Matter **24**, 225501 (2012).

[16] See Supplemental Material at http://link.aps.org/supplemental/10.1103/PhysRevLett.118.025701 for simulation method and videos with typical phase transformation processes, which includes Refs. [17–32].

[17] P. Steve, Fast parallel algorithms for short-range molecular dynamics, J. Comput. Phys. **117**, 1 (1995).

[18] M. J. Buehler, A. C. van Duin, and W. A. Goddard III, Multiparadigm Modeling of Dynamical Crack Propagation in Silicon Using a Reactive Force Field, Phys. Rev. Lett. **96**, 095505 (2006).

[19] M. J. Buehler, H. Tang, A. C. van Duin, and W. A. Goddard III, Threshold Crack Speed Controls Dynamical Fracture of Silicon Single Crystals, Phys. Rev. Lett. **99**, 165502 (2007).

[20] U. Khalilov, E. C. Neyts, G. Pourtois, and A. C. van Duin, Can we control the thickness of ultrathin silica layers by hyperthermal silicon oxidation at room temperature?, J. Phys. Chem. C **115**, 24839 (2011).

[21] S. Dumpala, S. R. Broderick, U. Khalilov, E. C. Neyts, A. C. van Duin, J. Provine, R. T. Howe, and K. Rajan, Integrated atomistic chemical imaging and reactive force field molecular dynamic simulations on silicon oxidation, Appl. Phys. Lett. **106**, 011602 (2015).

[22] M. I. Baskes, Modified embedded-atom potentials for cubic materials and impurities, Phys. Rev. B **46**, 2727 (1992).

[23] F. H. Stillinger and T. A. Weber, Computer simulation of local order in condensed phases of silicon, Phys. Rev. B **31**, 5262 (1985).

[24] P. Erhart and K. Albe, Analytical potential for atomistic simulations of silicon, carbon, and silicon carbide, Phys. Rev. B **71**, 035211 (2005).

[25] H. Balamane, Comparative study of silicon empirical interatomic potentials, Phys. Rev. B **46**, 2250 (1992).

[26] M. D. Kluge, J. R. Ray, and A. Rahman, Amorphous-silicon formation by rapid quenching: A molecular-dynamics study, Phys. Rev. B **36**, 4234 (1987).

[27] G. Mogni, A. Higginbotham, K. Gal-Nagy, N. Park, and J. S. Wark, Molecular dynamics simulations of shock-compressed single-crystal silicon, Phys. Rev. B **89**, 064104 (2014).

[28] V. Domnich, D. Ge, and Yu. Gogotsi, *Indentation-Induced Phase Transformations in Semiconductors, In: High Pressure Surface Science and Engineering*, edited by Y. Gogotsi and V. Domnich (Institute of Physics, Bristol, 2004), Section V.1, pp. 381–442.

[29] M. Durandurdu, Diamond to β-Sn phase transition of silicon under hydrostatic and nonhydrostatic compressions, J. Phys. Condens. Matter **20**, 325232 (2008).

[30] H. J. Berendsen, J. V. Pstma, van Gunsteren, W. F. DiNola, and J. R. Haak, Molecular dynamics with coupling to an external bath, J. Chem. Phys. **81**, 3684 (1984).

[31] A. K. Suhramaniyan, Int. J. Solids Struct. **45**, 4040 (2008).

[32] A. Stukowski, Visualization and analysis of atomistic simulation data with OVITO–the Open Visualization Tool, Model. Simul. Mater. Sci. Eng. **18**, 015012 (2010).

[33] V. I. Levitas and K. Samani, Melting and solidification of nanoparticles: Scale effects, thermally activated surface nucleation, and bistable states, Phys. Rev. B **89**, 075427 (2014).

[34] V. I. Levitas and M. Javanbakht, Surface-Induced Phase Transformations: Multiple Scale and Mechanics Effects and Morphological Transitions, Phys. Rev. Lett. **107**, 175701 (2011).

[35] V. I. Levitas and M. Javanbakht, Advanced phase-field approach to dislocation evolution, Phys. Rev. B **86**, 140101(R) (2012).

[36] K. Momeni, V. I. Levitas, and J. A. Warren, The strong influence of internal stresses on the nucleation of a nano-sized, deeply undercooled melt at a solid—solid phase interface, Nano Lett. **15**, 2298 (2015).

[37] V. I. Levitas and A. M. Roy, Multiphase phase field theory for temperature-induced phase transformations: Formulation and application to interfacial phases, Acta Mater. **105**, 244 (2016).